*** Manuscript IN PRESS at JOURNAL OF NEUROPHYSIOLOGY as of 7/08/2014 ***

RUNNING HEAD: **Pre-stimulation phase predicts the TMS-evoked response**

# Pre-stimulation phase predicts the TMS-evoked response

Bornali Kundu[1], Jeffrey S. Johnson[2], Bradley R. Postle[2,3]

1. Medical Scientist Training Program and the Neuroscience Training Program, University of Wisconsin—Madison, USA
2. Department of Psychiatry, University of Wisconsin—Madison, USA
3. Department of Psychology, University of Wisconsin—Madison, USA

Corresponding Author:

Bornali Kundu
Department of Psychiatry
University of Wisconsin-Madison
6001 Research Park Blvd.
Madison, WI 53719

Phone: 1-608-265-8961
Email: bkundu@wisc.edu

**ABSTRACT**

Pre-stimulation oscillatory phase and power in particular frequency bands predict perception of at-threshold visual stimuli and of transcranial magnetic stimulation (TMS)-induced phosphenes. These effects may be due to changes in cortical excitability, such that certain ranges of power and/or phase values result in a state in which a particular brain area is more receptive to input, thereby biasing behavior. However, the effects of trial-by-trial fluctuations in phase and power of ongoing oscillations on the brain's electrical response to TMS itself have thus far not been addressed. The present study adopts a combined TMS and electroencepalography (EEG) approach to determine whether the TMS-evoked response is sensitive to momentary fluctuations in pre-stimulation phase and/or power in different frequency bands. Specifically, TMS was applied to superior parietal lobule while subjects performed a short-term memory task. Results showed that the pre-stimulation phase, particularly within the beta (15-25Hz) band predicted pulse-by-pulse variations in the global mean field amplitude. No such relationship was observed between pre-stimulation power and the global mean field amplitude. Furthermore, TMS-evoked power in the beta band fluctuated with pre-stimulation phase in the beta band in a manner that differed from spontaneous brain activity. These effects were observed in areas at and distal to the stimulation site. Together, these results confirm the idea that fluctuating phase of ongoing neuronal oscillations create "windows of excitability" in the brain, and they give insight into how TMS interacts with ongoing brain activity on a pulse-by-pulse basis.

Keywords: Transcranial magnetic stimulation (TMS), electroencephalography (EEG), phase, power, excitability

## INTRODUCTION

Spontaneous fluctuations in ongoing brain activity have been shown to exist within well-defined networks and have been linked to behavior (Schroeder and Lakatos, 2009; Palva and Palva, 2011). For example, the prestimulus phase and power of oscillations in the alpha frequency band (ranging from 8-14 Hz) recorded at occipital channels have been shown to predict the perception of at-threshold visual stimuli (Van Dijk et al., 2008; Mathewson et al., 2009; Wyart and Tallon-Baudry, 2009). These studies lend credence to the proposal that the brain's self-generated oscillations create a temporal context for the brain's network connectivity to behave under and respond to, which then translates into behavioral output (Buszáki, 2004). Generally, across studies, low prestimulus power has been found to predict signal detection, and high power predicts failure-to-detect (c.f. Babiloni et al., 2006). Additionally, low prestimulus alpha-band power (roughly defined as 8-12Hz) predicts higher amplitude of the blood-oxygen level-dependent (BOLD) response evoked by visual simulation (Scheeringa et al., 2009), as measured by functional magnetic resonance imaging (fMRI). The instantaneous phase, windowed to encompass the time interval immediately prior to stimulus onset, also predicts the probability of stimulus detection. In the case of alpha-band oscillations, the neural bases of these effects have been proposed to reflect the "pulsed-inhibition" of ongoing neural activity (Mathewson et al., 2009), a corollary of the idea that ensembles that oscillate in the alpha frequency range can no longer effectively process information (Jensen and Mazaheri, 2010). In another line of research, Lange and

colleagues (2013) used visual illusions to test whether prestimulus alpha-band power related to veridical perception. They found that low prestimulus alpha-band power was a better indicator of whether a subject reported a stimulus than of veridical perception per se. They, along with others, suggest that prestimulus alpha-band power might determine instantaneous cortical excitability, and that this state of excitability is subject to change moment-by-moment. In this context, excitability implies a momentary brain state in which, for example, visual cortex is more receptive to input from another brain area.

Another line of work, in the nonhuman primate, has implicated a role for oscillations in the beta band (roughly 15-25Hz) in “clocking” behavioral functions such as shifts of attention and the generation of eye movements (Buschman et al., 2009). The beta-band may also be an important frequency band for the implementation of top-down control via long-range phase synchronization (Engel and Fries, 2010).

Transcranial magnetic stimulation (TMS) can be used to induce weak electrical currents in targeted tissues, thereby altering ongoing neural activity (Walsh and Pascual-Leone, 2005). Incorporating TMS with electroencephalography (EEG) has made it possible to directly observe the effects of TMS on this activity. TMS of visual cortex at particular intensities can induce the perception of phosphenes, a phenomenon characterized by the subjective experience of brief light flashes in the absence of light entering the eye. The probability of TMS-induced phosphene perception has been used to operationalize cortical excitability in humans, and the probability of a subject

reporting TMS-induced phosphenes is correlated with trial-by-trial fluctuations in the pre-stimulation power (Romei et al., 2008) and phase (Dugué et al., 2011) of alpha-band oscillations. These studies suggest that TMS may interact with underlying brain oscillations such that the phase and power of these oscillations predict the effects of TMS on subsequent behavior. Romei and colleagues (2010) suggest that signal detection may depend on fluctuations in cortical excitability, such that low pre-stimulation alpha-band power is thought to correspond to a state in which the cortex is more receptive to input, in this case, by TMS-induced current.

A limitation of task-related visual perception and of phosphene perception, however, is that both are indirect measures of cortical excitability and connectivity, in that they, presumably, reflect the result of several electrophysiological steps after stimulation. What does "increased excitability" look like at the network level, in the whole brain? One way to investigate this is to assess whether the TMS evoked response (TMS-ER) itself is influenced by the pre-stimulation phase and/or power. Unfortunately, in the case of the phosphene perception paradigm, the visual evoked potential (VEP) produced by visual cortex as a result of perceiving the phosphene will necessarily confound the measurement of the TMS-ER itself. Thus, in the present study, we investigated whether trial-by-trial variations in pre-stimulation phase and/or power influenced properties of the TMS-ER to single pulses delivered to the superior parietal lobule (SPL) during the delay period of a spatial short-term memory (STM) task. The data were drawn from a previously published study which showed that the

TMS-ER differed depending on whether TMS was applied during the performance of the STM task versus during a perceptually identical period of fixation (Johnson et al., 2012). Crucially, the site of stimulation ensured that there was no perceptual evoked response from TMS in this task context.

Results revealed that spontaneous fluctuations in pre-stimulation phase within beta frequency band had a systematic effect on the amplitude and spectral properties of the TMS-ER. No such effects were found for pre-stimulation power. These findings provide direct support for the idea that moment-by-moment changes in underlying, spontaneous oscillations, as indexed by changes in pre-stimulation phase, perhaps more so than power, may drive trial-by-trial variations in behaviors, such as visual perception, through changes in cortical excitability and/or connectivity.

## METHODS

### Subjects

16 subjects recruited from the University of Wisconsin-Madison community participated in the study (8 males, mean age = 21.9 [SD=2.9]), described in Johnson et al. (2012). The study protocol was approved by the UW-Madison Health Sciences Institutional Review Board. All subjects gave written informed consent and were screened for neurological and psychiatric conditions and other risk factors related to the application of TMS prior to participation.

### Experimental Task and Procedure

Single pulses of TMS were delivered to the SPL during the delay period of a spatial STM task. Each trial of the task began with a 1000 ms fixation period

followed by the sequential presentation of four memory targets at different, randomly selected screen locations. Stimulus presentation was followed by a 3750 ms delay period, during which the central fixation cross remained visible, followed by the appearance of a probe stimulus that was present for up to 2000 ms (**Figure 1A**). When the probe appeared, subjects made a yes/no button press, indicating whether the location of the probe matched the location of any one of the four memory targets (50% probability). On 50% of trials (randomly interleaved), two TMS pulses were delivered at an average rate of 0.5 Hz during the delay period: The first pulse was delivered 750 ± 250 ms after delay-period onset (i.e., a minimum of 700 ms after the offset of the final memory array item), followed by the second pulse 2000 ± 250 ms later. Trials with TMS will be referred to as the $TMS_{on}$ trials/condition and trials without TMS will be referred to as the $TMS_{off}$ trials/condition. Trials were separated by a 1000 ms intertrial interval (ITI). A total of 160 TMS pulses were delivered across 80 $TMS_{on}$ trials, intermixed with an equal number of $TMS_{off}$ trials. Full details can be found in Johnson et al. (2012).

**TMS targeting and stimulation**

TMS was delivered with a Magstim Standard Rapid magnetic stimulator equipped with a 70-mm figure-of-eight stimulating coil (Magstim, Whitland, UK). TMS was applied to a portion of the left SPL [Brodmann's Area (BA) 7] dorsal and medial to the intraparietal sulcus and posterior to the postcentral sulcus (**Figure 1A inset**). The SPL was identified on the basis of individual anatomy from whole-brain T1-weighted anatomical MRIs that were acquired with a GE

MR750 3T MRI scanner for each subject prior to the study (176 axial slices with a resolution of 1 mm). TMS targeting was achieved using a Navigated Brain Stimulation (NBS) system (Nextstim, Helsinki, Finland) that uses infrared-based frameless stereotaxy to map the position of the coil and the subject's head within the reference space of the individual's high-resolution MRI. TMS was delivered at an intensity of 110-140 V/m (for a given subject, intensity and coil position were held constant across the task; Rosanova et al., 2009; Casali et al., 2010). Maximum stimulator output varied from 65% to 92% (M=82%, SD=9%). Pulses were biphasic with a pulse-duration of 0.280 ms. To avoid contamination of the EEG by auditory artifacts, masking noise was played through inserted earplugs throughout the testing session, as in previous studies (Esser et al., 2006).

**EEG recording**

EEG was recorded with a 60-channel TMS-compatible amplifier (Nexstim; Helenski, Finland), which uses a sample-and-hold circuit that holds amplifier output constant from 100 μs pre- to 2 ms post-stimulus. Electrode impedance was kept below 3kΩ. There was a 0.1 Hz high-pass filter built into the amplifier. A single electrode, placed on the forehead, was used as the reference and eye movements were recorded with two additional electrodes placed near the eyes. Data were sampled at 1450 Hz with 16-bit resolution.

**Data preprocessing**

Data were processed offline using the EEGLab toolbox (Delorme and Makeig, 2004) running MATLAB R2012b (Mathworks, Natick, MA, USA). The data were downsampled to 500 Hz, band-pass filtered between 2-80 Hz, and

notch filtered at 60 Hz. Movement-related artifacts were identified and removed by visual inspection and individual electrodes exhibiting excessive noise were reinterpolated using spherical spline interpolation. All data were average-referenced. Independent components analysis was then used to identify and remove components reflecting residual muscle activity, eye movements, blink-related activity, and residual TMS-related artifacts. Eye movements, blinks, and muscle artifacts were detected using standard procedures as described in (Jung et al., 2000). TMS artifacts were identified and removed as described in Hamidi et al. (2010). Greater than 91% of trials (roughly 146/160 trials per subject) remained after removal of trials containing large artifacts, resulting in an average of 146 (*SD* = 18) TMS pulses available for analysis per subject after data processing.

**Analysis Methods**

**Overview**. The goal of the study was to determine if the power or phase immediately prior to TMS predicted the amplitude and/or extent of propagation of the TMS-ER on a trial-by-trial basis. We approached the problem using a two-step process. The rationale for Step 1 was that, because specific frequencies involved in determining these properties of the TMS-ER were not known a priori, we would first empirically determine candidate frequencies based on the aspects of the EEG signal that accounted for variation in the TMS-ER. Having done so, Step 2 would characterize how pre-stimulation phase at the frequencies identified in Step 1 influenced spectral properties of the TMS-ER measured across the scalp.

To begin Step 1, trials were sorted by a measure of brain activation that captures the global amplitude and spread of the TMS-ER, the global mean field amplitude (GMFA, Lehmann and Skrandies, 1980; Komssi et al., 2004). We then determined which frequencies showed the greatest difference in power or intertrial phase coherence (ITC, Tallon-Baudry et al., 1996) prior to TMS using GMFA as a dependent categorical variable. Specifically, we labeled the GMFA as being either 'high' or 'low' relative to the median value (**Figure 1B**). Based on the assumption that EEG signals are derived from fluctuations in local field potentials of cortical ensembles, we assumed that oscillatory sources generating coherent signal (showing higher ITC) in particular frequency bands would have greater collective influence on the subsequent TMS-ER than non-coherent sources (i.e. those showing relatively low ITC; Pesaran et al., 2002; Tallon-Baudry et al., 2004). Additionally, sources generating signal with high power in certain frequencies were assumed to have more 'potential energy' to subsequently influence the TMS-ER than sources generating low amounts of power. It may be the case that these sources are composed of more neural elements as well. Thus, relatively low power was interpreted to mean that the relative size of the underlying neural ensemble was either smaller or less activated pre-stimulation, and thus would not have as much of an influence on the TMS-ER (quantified at the scalp-level as the GMFA).

Step 2 of the analysis was more exploratory in nature, and involved characterizing how pre-stimulation phase at the frequencies identified in Step 1 influenced spectral properties of the TMS-ER measured across the scalp. (Note

that, because pre-stimulation power was not found to predict the GMFA in Step 1, power was not addressed in Step 2.) To do so, we assessed the trial-by-trial variations in "post-TMS" power by re-sorting all trials now according to prestimulus phase and the frequency and time points pre-stimulation, defined by Step 1, and determining the effect of phase on "post-TMS" power across conditions. These effects were compared to the EEG recorded during corresponding segments of a cognitively equivalent "no TMS" condition (the $TMS_{off}$ condition), in which participants completed the STM task in the absence of TMS. The post-TMS evoked power has been suggested to reflect resonance properties of cortico-thalamic circuits (Rosanova et al., 2009) and has been used as a measure of the 'state' of the stimulated cortical networks, specifically, the state of the network 'effective connectivity' (Casali et al., 2010).

**Procedures**

**Step 1**. To determine which frequencies influenced the TMS-ER, we calculated the GMFA, as follows (based on Lehmann & Skrandies, 1980):

$$GMFA(t) = \sqrt{\left[\sum_{i}^{k}(V_i(t) - V_{mean}(t))^2\right]/k}$$

where *t* is the time point in the trial, *i* is the current electrode, and *k* is the total number of electrodes. The GMFA was calculated from 10-400 ms post-TMS. We then sorted each subjects' trials via median split into those with 'high' or 'low' GMFA (High and Low groups, **Figure 1B**). Because TMS was delivered near to channel P1, the pre-stimulation ITC and power were calculated for each

frequency, for High and Low GMFA groups, at this channel. Both were derived from a time-frequency transformation of the data using Hanning tapers with a frequency-dependent window of 3 cycles/frequency analyzed, calculated from 2-50 Hz. Three cycles were chosen because this is the minimum number required to obtain a reliable measure of the 'instantaneous phase' (Le Van Quyen et al., 2001) while still allowing estimation of phase and power in the pre-TMS interval uncontaminated by the pulse itself. (Note that this restricts the pre-stimulation time-window of observation to effectively 1.5 cycles per frequency of interest.) The difference between High and Low GMFA groups was compared to a surrogate distribution of difference values (power difference between High and Low GMFA groups, or ITC difference between High and Low GMFA groups) obtained through a bootstrapping procedure as follows. For each subject, trials were randomly assigned to one of two groups and a difference in power and ITC was calculated for channel P1 data. This was repeated 10,000 times per subject. From this, a grand average distribution was derived by selecting a difference sample from each subjects' surrogate distribution, and calculating a grand average difference in power or ITC. This procedure was also repeated 10,000 times. Finally, we identified clusters of frequency-time points pre-stimulation that showed significant differences in power or ITC (between High and Low GMFA bins) relative to this surrogate distribution, with significance differences defined as those samples showing less than 5% of null samples to be above the experimental sample (similar to $p<0.05$). To correct for multiple comparisons, we also identified clusters of frequency-time points that were corrected considering a

false discovery rate (FDR) of 5% (Benjamini and Hochberg, 1995). Note that, due to the nature of EEG-derived spectrograms, however, each test is not truly independent of all the others so this correction is overly conservative, thus we present both sets of results (corrected and uncorrected).

***Step 2.*** Having determined that the pre-stimulation phase at 20Hz and -150ms (defined by the results from Step 1, see **Figure 2A**) predicts the amplitude of the GMFA, in the second part of the analysis, we sought to characterize the relationship between pre-stimulation phase at this frequency and time point and the spectral properties of the TMS-ER in the beta band. We calculated the pre-stimulation phase of data derived from channel P1. As above, the time-frequency representation of the data was derived using Hanning tapers and a window length of 3 cycles, at 20Hz and -150ms. Because the analysis was focused on discovering patterns in the data, as opposed to testing a priori predictions about the effects of stimulating at particular phase angles, the data were binned into 10 phase bins (36 degrees each). To analyze spectral properties of the TMS-ER within each bin, we calculated the average power from 10-400 ms after TMS onset for each bin (using Hanning tapers, window length 3 cycles; evaluated from 15-25 Hz), referred to as the 'TMS-evoked power'. To determine if prestimulus phase had a significant effect on the TMS-ER, we compared these data to the "null result", the $TMS_{off}$ condition, which captures the naturally present relationship between ongoing phase and power fluctuations in oscillatory activity. In other words, we accounted for the relationship one might expect to exist between power and phase at one time point and the power of the

signal at a subsequent time point, absent the delivery of TMS. To do this, trials from the $TMS_{off}$ condition were epoched into two sub-trials per delay period similar to the $TMS_{on}$ condition, such that one set of sub-trials was centered at 750 ± 250 ms after delay onset, and an equal number at a second time point 2000 ± 250 ms after that. For each condition, power in the 10-400 ms time window will be referred to as the 'post-stimulation' power, even though no TMS pulses were delivered in the $TMS_{off}$ condition. Similarly, the phase before time 0 ms will be referred to as 'pre-stimulation' phase. Because the pattern of effects is not known a priori, we chose to use a two-way analysis of variance (ANOVA) with phase bin (1-10) and TMS (on and off) as within Subject factors, to determine if pre-stimulation phase at a particular channel predicted post-stimulation power in the beta band. Bonferroni correction (Type 1 error $\alpha$=0.05) was done for multiple comparisons, though note that this test is not optimal for these data since the electrodes are contiguous in space, and thus the tests are not truly independent.

## RESULTS

All subjects showed a significant difference in mean GMFA between High and Low post-stimulation GMFA conditions (two-sided unpaired *t*-tests, ps<0.05; **Figure 1B**), confirming the validity of using this procedure to obtain an outcome measure for the subsequent analyses. Note there was no significant effect of TMS on performance accuracy of the spatial STM task (mean % accuracy on $TMS_{on}$ trials was 84.38 (*SD*=8.37) and on $TMS_{off}$ trials was 84.06 (*SD*=8.75); *p*>0.99; Johnson et al., 2012). Furthermore, there was no effect of pulse position (pulse 1 versus 2) on the categorization of GMFA (one-way ANOVA with subject

as a repeated measure, $F$=1.3; $p$=0.26). We will first describe the effects of the pre-stimulation phase on the TMS-ER (Step 1 and Step 2 analyses), followed by consideration of the effects of pre-stimulation power on the TMS-ER (Step 1 only).

**The TMS-ER is influenced by the pre-stimulation oscillatory phase**

For Step 1 of the analyses, we found that pre-stimulation phase in the beta and gamma bands predicted the amplitude of the TMS-ER, as measured using GMFA. Results indicated that the ITC from 15-25 Hz (-200 to -150ms) pre-TMS, corresponding to the beta band, and from 33-41Hz (-330 to -280ms) and from 33-50Hz (-180 to -80ms) pre-TMS, corresponding to the gamma band, predicted whether the GMFA would be High or Low (all ps≤0.05, uncorrected; **Figure 2A**). Elevated phase coherence in these bands and time points predicted elevated GMFA from 10-400 ms post-TMS (i.e., the duration of the TMS-ER). The effect was present for each frequency within those bands (i.e., effects were present over continuous frequencies and time points). After FDR correction, one cluster remained in the beta band (all ps≤0.05, corrected; **Figure 2A**).

Using this information, in Step 2 of the analysis, we determined that, for $TMS_{on}$ trials, post-stimulation power in the beta band showed maximal amplitude at particular phases at 20Hz and at -150ms (point within the cluster that survived multiple comparisons testing, **Figure 2A**), and these phases differed from those underlying the relationship between beta band power and phase in the $TMS_{off}$ condition. We needed to account for temporal dependencies of sorting by pre-stimulation phase, because it is likely that there is a relationship between phase

at one time point and a later time point, regardless of the influence of TMS. To do this, we compared the $TMS_{on}$ condition to the cognitively equivalent $TMS_{off}$ condition (i.e. the TMS × Phase Bin interaction; see **Methods**). This analysis revealed a significant effect of pre-stimulation phase at 20Hz on post-stimulation power in the beta band in a cluster of central, parietal and occipital electrodes that are relatively continuous in space (channels FCz, CP3, CP1, CPz, P3, P1, Pz, PO3, POz, PO4, O1, Oz, O2, and Iz; **Table 1**, **Figure 3A**). There was a main effect of TMS at channels AF3, AFz, F1, Fz, F2, FC1, FCz, FC2, Cz, C6, TP9, CP1, CPz, CP2, TP10, P1-P8, Pz, PO3, POz, PO4, O1, Oz, O2, and Iz (*ps*≤0.05, **Table 1**). There was a main effect of phase at channels AFz, AF4, Fz, F2, FC2, P3, P5, PO3, and O1 (*ps*≤0.05, **Table 1**). The abovementioned channels showed a significant TMS x Phase Bin interaction (*ps*≤0.05, **Table 1**). On visual inspection of the data, the pattern of this effect across phase bins was qualitatively similar across these channels (**Figures 3 B and C)**. Post-stimulation power was elevated relative to power in the $TMS_{off}$ condition, when the pre-stimulation phase in the beta band was between -4π/5 radians to -3π/5 radians (-143° to -108°) and between π/5 radians to 2π/5 radians (37° to 72°). Note the phase of the sorting frequency is shown as a 'descriptive cycle' on the cumulative plot shown in **Figure 3C** for illustration.

**The TMS-ER is not influenced by pre-stimulation oscillatory power**

Pre-stimulation power did not predict the magnitude of the TMS-ER as quantified by the GMFA. Results showed no significant effects within the time windows allotted for this analysis (**Figure 2B**). Because no significant clusters

were found in the Step 1 analyses, Step 2 analyses were not performed for pre-stimulation power.

## DISCUSSION

The present study sought to find elements of the ongoing EEG that relate to the brain's momentary state of excitability and connectivity, as measured by the TMS-ER. Specifically, we investigated whether trial-by-trial variation in pre-stimulation phase or power at the site of TMS predicted subsequent variations in one measure of brain activation, the TMS-ER, which is sensitive to global brain states such as sleep stages (Massimini et al., 2005), levels of clinically-determined consciousness (Rosanova et al., 2012), and cognitive context (Johnson et al., 2012). The present report describes results of an analysis of data from Johnson et al. (2012) at a finer temporal scale than has previously been studied. Specifically, we investigated whether the TMS-ER was sensitive to moment-by-moment fluctuations in oscillatory activity during STM, as measured by the pre-stimulation phase and power across frequency bands. This question has been previously addressed during non-rapid eye movement sleep using frequencies <1 Hz (Bergmann et al., 2012), but not during an awake, task state.

At the whole-brain level, results obtained in Step 1 of the analysis revealed that pre-stimulation phase in the beta and gamma frequency bands predicted the global amplitude of the TMS-ER, summarized by the GMFA. Only the beta band cluster survived a test of multiple comparisons. In contrast, we found no reliable relationship between pre-stimulation power and the GMFA in any frequency band. Follow-up analysis showed that TMS-evoked power in the

beta band had maximal amplitude when pre-stimulation (-150 ms) phase at 20Hz was between -4π/5 radians to -3π/5 radians (-143° to -108°) and between π/5 radians to 2π/5 radians (37° to 72°). This roughly corresponds to the rising and falling slopes of a cosine curve. To our knowledge, this observation reflects a previously un-described means by which TMS influences ongoing brain activity. This pattern of effects was distributed across central, parietal and occipital channels. These results provide evidence supporting the proposal that the brain's internally generated rhythms create a meaningful temporal context that determines the immediate, instantaneous brain state, as measured by the TMS-ER. Intriguingly, Monto et al. (2008) have shown that infraslow oscillations (0.01 Hz to 0.1 Hz) organize all other spectral frequencies, which reach their peaks at –π/2 radians of the infraslow oscillations. This property is also reflected in behavioral performance peaks. Such infraslow oscillations, it is suggested, might influence the general excitability of cortical networks. Somewhat relatedly, it has been shown in rats that LTP can be induced when high-frequency bursts are applied at the post-stimulation peaks of the stimulus-induced phase reset theta wave, but not at the troughs (Anwyl and Rowan, 1997). Although at present this is little more than speculation, these effects might account for why, in the present study, the TMS-ER was largest at the rising and falling phase-to-peak of the sorting (beta band) frequency. It is important to keep in mind, however, that the observations made in the Step 2 analysis are preliminary, and require follow-up in a properly designed experiment with greater numbers of trials. In general, the origin of high frequency oscillations, such as the beta and gamma bands, are not

known, and furthermore, it is not known how polarity shifts might change with recording electrode and reference position.

The sensitivity of the TMS-ER to pre-stimulation phase is in line with the general theory that underlying oscillations produce fluctuations in cortical excitability (Bishop, 1933; Buzsáki and Draguhn, 2004). A related possibility, particularly relevant for our Step 2 analysis, is that these results reflect increased communication between distal brain regions, without involving an increase in excitability per se. For example, it is possible that a distal region could be at an equivalent level of excitability on two trials, but if the inputs are more effectively phase-synchronized on trial B than on trial A, that the evoked response to B would be greater. These two possibilities are by no means mutually exclusive. By either explanation, our data support the proposal that fluctuation in the phase of an underlying oscillation effectively creates 'windows of excitability' during which the brain, or a particular brain area, is in a state that is more open to perturbation or communication with other brain areas (Dugué et al., 2011). We find that this is literally true in the context of TMS. The TMS-evoked power in the beta band is larger when TMS is delivered at particular phases of that band. In the context of a subject performing a STM task, pre-stimulation phase in the beta band predicted subsequent effects in the post-stimulation beta band power.

Interestingly, we did not find a significant relationship between pre-stimulation power and GMFA. Although either of these findings may seem to be at odds with some of the literature reviewed in the introduction, there are important methodological differences to keep in mind. One feature of the present

study was the restricted time window during which we could assess pre-stimulation effects: from 500 ms prestimulation to 1.5 cycles (per frequency) prestimulation. Thus, we cannot rule out the possibility that effects of pre-stimulus power might be present in our data if power could have been estimated at time points closer to TMS delivery. As for comparison to studies using visual perception as the dependent measure, it may be that fluctuations in alpha-band power that predict such factors as phosphene and stimulus detection thresholds reflect relatively local dynamics within the occipital cortex, whereas the power fluctuations observed during a visual STM task, such as that featured in the present study, likely reflect long-range interactions between distal brain areas, including frontoparietal regions (Kundu et al., 2013). If this were the case, regional phase synchronizing long-range connectivity would be more pronounced in the case of complex tasks such as STM compared to relatively regional phenomena such as visual perception.

In general, the results from the present study provide empirical support for theoretical accounts that fluctuating phase of ongoing oscillations create 'windows of excitability' in the brain. Furthermore, they give insight into how TMS interacts with ongoing brain activity on a pulse-by-pulse basis. Thus, they are applicable to understanding the electrophysiological and biological underpinnings of studies using single-pulse as well as repetitive TMS for a wide range of applications, from basic science to medicine.

**Grants**

This study was supported by grants MH095428 (B.K.), MH88115 (J.S.J.), and MH064498 and MH095984 (B.R.P.) from the National Institute of Mental Health.

## Disclosure/Conflict of Interest

The authors declare that the research described here was conducted in the absence of any commercial or financial relationships that could be construed as a potential conflict of interest.

## Author Contributions

B.K., J.S.J. and B.R.P. conceived of and designed the research; B.K. and J.S.J. performed experiments; B.K. analyzed data and interpreted results of experiments; B.K., J.S.J., and B.R.P. drafted manuscript.

## Acknowledgements

We would like to thank Dr. Olivia Gosseries for her thoughtful comments regarding the manuscript.

## REFERENCES


**Anwyl R, Rowan MJ**. Stimulation on the Positive Phase of Hippocampal Theta Rhythm Induces Long-Term Potentiation That Can Be Depotentiated by Stimulation on the Negative Phase in Area CA1 In Vivo Christian Ho. *J Neurosci* 17: 6470–6477, 1997.

**Babiloni C, Vecchio F, Bultrini A, Luca Romani G, Rossini PM**. Pre- and poststimulus alpha rhythms are related to conscious visual perception: a high-resolution EEG study. *Cereb. Cortex* 16: 1690–700, 2006.

**Benjamini Y, Hochberg Y**. Controlling the false discovery rate: a practice and powerful approach to multiple testing. *J. R. Stat. Soc. Ser. B* 57: 289–300, 1995.

**Bergmann TO, Mölle M, Schmidt M a, Lindner C, Marshall L, Born J, Siebner HR**. EEG-guided transcranial magnetic stimulation reveals rapid shifts in motor cortical excitability during the human sleep slow oscillation. *J. Neurosci.* 32: 243–53, 2012.

**Bishop GH**. Cyclic changes in excitability of the optic pathway of the rabbit. *Am J Psychiatry* 103: 213–224, 1933.

**Busch NA, Dubois J, VanRullen R**. The phase of ongoing oscillations predicts visual perception. *J. Neurosci.* 31: 11889–93, 2011.

**Busch NA, VanRullen R**. Spontaneous EEG oscillations reveal periodic sampling of visual attention. *Proc. Natl. Acad. Sci. U. S. A.* 107: 16048–53, 2010.

**Bushman TJ and Miller EK.** Serial, covert shifts of attention during visual search are reflected by the frontal eye fields and correlated with population oscillations. *Neuron* 63:386-96

**Buzsáki G, Draguhn A**. Neuronal oscillations in cortical networks. *Science* 304: 1926–9, 2004.

**Casali AG, Casarotto S, Rosanova M, Mariotti M, Massimini M**. General indices to characterize the electrical response of the cerebral cortex to TMS. *Neuroimage* 49: 1459–1468, 2010.

**Delorme A, Makeig S**. EEGLAB: an open source toolbox for analysis of single-trial EEG dynamics including independent component analysis. *J. Neurosci. Methods* 134: 9–21, 2004.

**Van Dijk H, Schoffelen J-M, Oostenveld R, Jensen O**. Prestimulus oscillatory activity in the alpha band predicts visual discrimination ability. *J. Neurosci.* 28: 1816–23, 2008.

**Dugué L, Marque P, VanRullen R**. The phase of ongoing oscillations mediates the causal relation between brain excitation and visual perception. *J. Neurosci.* 31: 11889–93, 2011.

**Engel AK and Fries P**. Beta band oscillations - signalling the status quo. *Curr Opin in Neurobio*. 20: 156-65. 2010

**Esser SK, Huber R, Massimini MJ, Peterson MJ, Ferarelli F, Tononi G.** A direct demonstration of cortical LTP in humans: a combined TMS/EEG study. *Brain Res Bull*. 69(1): 86-94. 2006

**Hamidi M, Slagter HA, Tononi G, Postle BR**. Brain responses evoked by high-frequency repetitive transcranial magnetic stimulation: An event-related potential study. *Brain Stimul.* 3: 2–14, 2010.

**Jensen O, Mazaheri A**. Shaping functional architecture by oscillatory alpha activity: gating by inhibition. *Front. Hum. Neurosci.* 4: 186, 2010.

**Johnson JS, Kundu B, Casali AG, Postle BR**. Task-dependent changes in cortical excitability and effective connectivity: A combined TMS-EEG study. *J. Neurophysiol.* 107: 2383–2392, 2012.

**Jung TP, Makeig S, Humphries C, Lee TW, McKeown MJ, Iragui V, Sejnowski TJ**. Removing electroencephalographic artifacts by blind source separation. *Psychophysiol.* 37: 163–78, 2000.

**Komssi S, Kähkönen S, Ilmoniemi RJ**. The effect of stimulus intensity on brain responses evoked by transcranial magnetic stimulation. *Hum. Brain Mapp.* 21: 154–64, 2004.

**Kundu B, Sutterer DW, Emrich SM, Postle BR.** Strengthened effective connectivity underlies transfer of working memory training to tests of short-term memory and attention. *J Neurosci*. 33(20): 8705-15, 2013.

**Lange J, Oostenveld R, Fries P**. Reduced Occipital Alpha Power Indexes Enhanced Excitability Rather than Improved Visual Perception. *J. Neurosci.* 33: 3212–3220, 2013.

**Lehmann D, Skrandies W**. Reference-free identification of components of checkerboard-evoked multichannel potential fields. *Electroencephalogr. Clin. Neurophysiol.* 48: 609–21, 1980.

**Massimini M, Ferrarelli F, Huber R, Esser SK, Singh H, Tononi G**. Breakdown of cortical effective connectivity during sleep. *Science* 309: 2228–2232, 2005.

**Mathewson KE, Gratton G, Fabiani M, Beck DM, Ro T**. To see or not to see: prestimulus alpha phase predicts visual awareness. *J. Neurosci.* 29: 2725–32, 2009.

**Monto S, Palva S, Voipio J, Palva JM**. Very slow EEG fluctuations predict the dynamics of stimulus detection and oscillation amplitudes in humans. *J. Neurosci.* 28: 8268–72, 2008.

**Palva S, Palva JM**. Functional roles of alpha-band phase synchronization in local and large-scale cortical networks. *Front. Psychol.* 2: 204, 2011.

**Pesaran B, Pezaris JS, Sahani M, Mitra PP, Andersen R a**. Temporal structure in neuronal activity during working memory in macaque parietal cortex. *Nat. Neurosci.* 5: 805–11, 2002.

**Romei V, Brodbeck V, Michel C, Amedi A, Pascual-Leone A, Thut G**. Spontaneous fluctuations in posterior alpha-band EEG activity reflect variability in excitability of human visual areas. *Cereb. Cortex* 18: 2010–8, 2008.

**Rosanova M, Casali A, Bellina V, Resta F, Mariotti M, Massimini M**. Natural frequencies of human corticothalamic circuits. *J. Neurosci.* 29: 7679–7685, 2009.

**Rosanova M, Gosseries O, Casarotto S, Boly M, Casali AG, Bruno M-AA, Mariotti M, Boveroux P, Tononi G, Laureys S, Massimini M**. Recovery of cortical effective connectivity and recovery of consciousness in vegetative patients. *Brain* 135: 1308–20, 2012.

**Scheeringa R, Petersson KM, Oostenveld R, Norris DG, Hagoort P, Bastiaansen MC**. Trial-by-trial coupling between EEG and BOLD identifies networks related to alpha and theta EEG power increases during working memory maintenance. *Neuroimage* 44: 1224–1238, 2009.

**Schroeder CE, Lakatos P**. Low-frequency neuronal oscillations as instruments of sensory selection. *Trends Neurosci.* 32: 9–18, 2009.

**Tallon-Baudry C, Bertrand O, Delpuech C, Pernier J**. Stimulus specificity of phase-locked and non-phase-locked 40 Hz visual responses in human. *J. Neurosci.* 16: 4240–9, 1996.

**Tallon-Baudry C, Mandon S, Freiwald W a, Kreiter AK**. Oscillatory synchrony in the monkey temporal lobe correlates with performance in a visual short-term memory task. *Cereb. Cortex* 14: 713–20, 2004.

**Le Van Quyen M, Foucher J, Lachaux J, Rodriguez E, Lutz A, Martinerie J, Varela FJ**. Comparison of Hilbert transform and wavelet methods for the analysis of neuronal synchrony. *J. Neurosci. Meth.* 111: 83–98, 2001.

**Walsh V, Pascual-leone A**. Transcranial Magnetic Stimulation: A Neurochronometrics of Mind (Bradford Books) MIT Press. 2003.

**Wyart V, Tallon-Baudry C**. How ongoing fluctuations in human visual cortex predict perceptual awareness: baseline shift versus decision bias. *J. Neurosci.* 29: 8715–25, 2009.

## FIGURE CAPTIONS

**Figure 1. A) Short-term memory task and experimental set-up.** Subjects performed a spatial STM task in which they were asked to remember the locations of the 4 shapes and indicate whether the probe's location matched a location of one of the targets. The shape of the targets is irrelevant to this task. TMS was applied to the SPL using MRI-guide stereotaxy. **B**) Global mean field amplitude (GMFA) in High and Low bins. The GMFA averaged over subjects, sorted into High (red trace) and Low (blue trace) bins. Width of ribbon denotes the standard error of the mean (SEM). TMS delivery at time 0ms (black line).

**Figure 2. Pre-stimulation phase or power and the GMFA. A**) The difference in ITC between groups of trials with either High or Low post-TMS GMFA. Clusters of time-frequency points that were significantly elevated above the null distribution shown where dashed lines delineate clusters with uncorrected p-values, solid lines delineate clusters with corrected p-values. The z-axis showed positive differences between high and low in red/warm colors and negative differences in blue/cool colors. **B**) Difference in power between High and Low GMFA trials. Same conventions as panel A. For both panels, the area delineated in white was not included in the analysis because of the possibility that it may contain contamination from the post-TMS time period due to windowing effects.

**Figure 3. Pre-stimulation phase at 20Hz relates to post-stimulation power in the beta band (15-25 Hz). A**) Topoplots of the difference between beta band

power for $TMS_{on}$ minus $TMS_{off}$ at each phase bin. Stars mark channels that showed a significant Phase Bin x TMS ($TMS_{on}$ versus $TMS_{off}$) interaction (*ps*≤0.05). **B**) Panels show the beta band power at each phase bin for channels that showed a significant Phase Bin x TMS ($TMS_{on}$ versus $TMS_{off}$) interaction. $TMS_{on}$ in red, $TMS_{off}$ in blue. 10 phase bins, from $-\pi$ to $\pi$, 36 degrees per bin. Standard 10-10 electrode channel layout used. **C**) Summary figure: mean post-stimulation beta band power across channels shown in panel B at each phase bin with descriptive cycle of the sorting frequency in dashed gray.

**Table 1. The effect of pre-stimulation phase at 20Hz on post-stimulation power in the beta (15-25 Hz) band across channels**

| Channel | Phase Bin | | TMS on | | Phase Bin x TMS on | |
|---|---|---|---|---|---|---|
| | *F(9,135)* | *p* | *F(1,15)* | *p* | *F(9,135)* | *p* |
| Fp1 | 0.890 | 0.536 | 3.453 | 0.083 | 0.724 | 0.686 |
| Fpz | 0.821 | 0.597 | 2.827 | 0.113 | 0.771 | 0.643 |
| Fp2 | 0.979 | 0.460 | 0.000 | 0.998 | 0.567 | 0.822 |
| AF3 | 1.534 | 0.142 | 4.540* | 0.050 | 0.960 | 0.476 |
| AFz | 1.949* | 0.050 | 7.268* | 0.017 | 1.280 | 0.253 |
| AF4 | 1.950* | 0.050 | 3.777 | 0.071 | 0.994 | 0.448 |
| F5 | 1.052 | 0.402 | 1.892 | 0.189 | 1.449 | 0.174 |
| F3 | 1.313 | 0.235 | 0.012 | 0.914 | 1.147 | 0.335 |
| F1 | 1.797 | 0.074 | 9.993* | 0.006 | 1.419 | 0.186 |
| Fz | 2.325* | 0.018 | 9.413* | 0.008 | 1.791 | 0.075 |
| F2 | 2.891* | 0.004 | 4.683* | 0.047 | 1.110 | 0.360 |
| F4 | 1.373 | 0.206 | 0.590 | 0.454 | 1.617 | 0.116 |
| F6 | 1.100 | 0.367 | 0.001 | 0.973 | 0.648 | 0.754 |
| FT9 | 1.275 | 0.256 | 0.080 | 0.782 | 1.092 | 0.373 |
| FT7 | 1.016 | 0.431 | 0.071 | 0.794 | 0.844 | 0.577 |
| FC5 | 1.022 | 0.426 | 0.250 | 0.624 | 1.067 | 0.391 |
| FC3 | 1.134 | 0.343 | 0.596 | 0.452 | 0.983 | 0.457 |
| FC1 | 1.287 | 0.250 | 8.433* | 0.011 | 0.908 | 0.520 |
| FCz | 1.700 | 0.095 | 9.060* | 0.009 | 2.317* | 0.019 |
| FC2 | 3.314* | 0.001 | 4.699* | 0.047 | 0.919 | 0.511 |
| FC4 | 1.121 | 0.352 | 0.774 | 0.393 | 0.897 | 0.530 |
| FC6 | 0.921 | 0.509 | 1.083 | 0.315 | 0.932 | 0.500 |
| FT8 | 1.206 | 0.296 | 0.983 | 0.337 | 1.030 | 0.419 |
| FT10 | 1.506 | 0.152 | 0.022 | 0.883 | 1.084 | 0.378 |
| T7 | 1.183 | 0.311 | 2.173 | 0.161 | 1.384 | 0.201 |
| C5 | 0.840 | 0.580 | 1.311 | 0.270 | 1.030 | 0.420 |
| C3 | 0.726 | 0.684 | 1.056 | 0.320 | 0.993 | 0.449 |
| C1 | 0.875 | 0.549 | 3.469 | 0.082 | 1.153 | 0.330 |
| Cz | 1.254 | 0.268 | 15.933* | 0.001 | 1.790 | 0.076 |
| C2 | 0.843 | 0.578 | 2.665 | 0.123 | 1.040 | 0.412 |
| C4 | 0.668 | 0.737 | 1.148 | 0.301 | 1.377 | 0.204 |
| C6 | 0.809 | 0.609 | 5.044* | 0.040 | 1.107 | 0.362 |
| T8 | 1.161 | 0.325 | 1.869 | 0.192 | 1.367 | 0.209 |
| TP9 | 0.917 | 0.512 | 5.144* | 0.039 | 1.487 | 0.159 |
| TP7 | 1.533 | 0.142 | 0.024 | 0.879 | 1.446 | 0.175 |
| CP5 | 1.249 | 0.271 | 0.485 | 0.497 | 1.625 | 0.114 |
| CP3 | 0.973 | 0.465 | 0.654 | 0.431 | 2.024* | 0.041 |
| CP1 | 1.180 | 0.313 | 10.033* | 0.006 | 2.105* | 0.033 |

| | | | | | | |
|---|---|---|---|---|---|---|
| CPz | 0.903 | 0.524 | 27.176* | 0.000 | 2.106* | 0.033 |
| CP2 | 0.538 | 0.845 | 4.738* | 0.046 | 1.640 | 0.110 |
| CP4 | 0.832 | 0.588 | 0.280 | 0.605 | 1.293 | 0.247 |
| CP6 | 1.873 | 0.061 | 0.855 | 0.370 | 1.416 | 0.187 |
| TP8 | 1.776 | 0.078 | 0.576 | 0.460 | 1.139 | 0.340 |
| TP10 | 0.877 | 0.547 | 5.452* | 0.034 | 1.137 | 0.341 |
| P7 | 1.194 | 0.304 | 10.824* | 0.005 | 1.575 | 0.129 |
| P5 | 2.233* | 0.023 | 12.186* | 0.003 | 1.755 | 0.082 |
| P3 | 1.961* | 0.049 | 10.379* | 0.006 | 2.721* | 0.006 |
| P1 | 1.665 | 0.103 | 7.588* | 0.015 | 2.184* | 0.027 |
| Pz | 0.465 | 0.896 | 5.817* | 0.029 | 2.222* | 0.024 |
| P2 | 0.741 | 0.671 | 5.245* | 0.037 | 1.621 | 0.115 |
| P4 | 1.193 | 0.304 | 5.985* | 0.027 | 1.195 | 0.303 |
| P6 | 1.421 | 0.185 | 6.296* | 0.024 | 1.106 | 0.363 |
| P8 | 1.652 | 0.107 | 3.938* | 0.066 | 1.508 | 0.151 |
| PO3 | 2.073* | 0.036 | 15.298* | 0.001 | 2.067* | 0.037 |
| Poz | 0.721 | 0.689 | 9.339* | 0.008 | 2.129* | 0.031 |
| PO4 | 0.845 | 0.576 | 7.450* | 0.016 | 1.953* | 0.050 |
| O1 | 2.811* | 0.005 | 10.458* | 0.006 | 2.002* | 0.044 |
| Oz | 1.223 | 0.286 | 12.891* | 0.003 | 2.499* | 0.011 |
| O2 | 1.164 | 0.323 | 4.321* | 0.055 | 1.992* | 0.045 |
| Iz | 1.503 | 0.153 | 16.464* | 0.001 | 2.353* | 0.017 |

* $p \leq 0.05$

# Figure 1

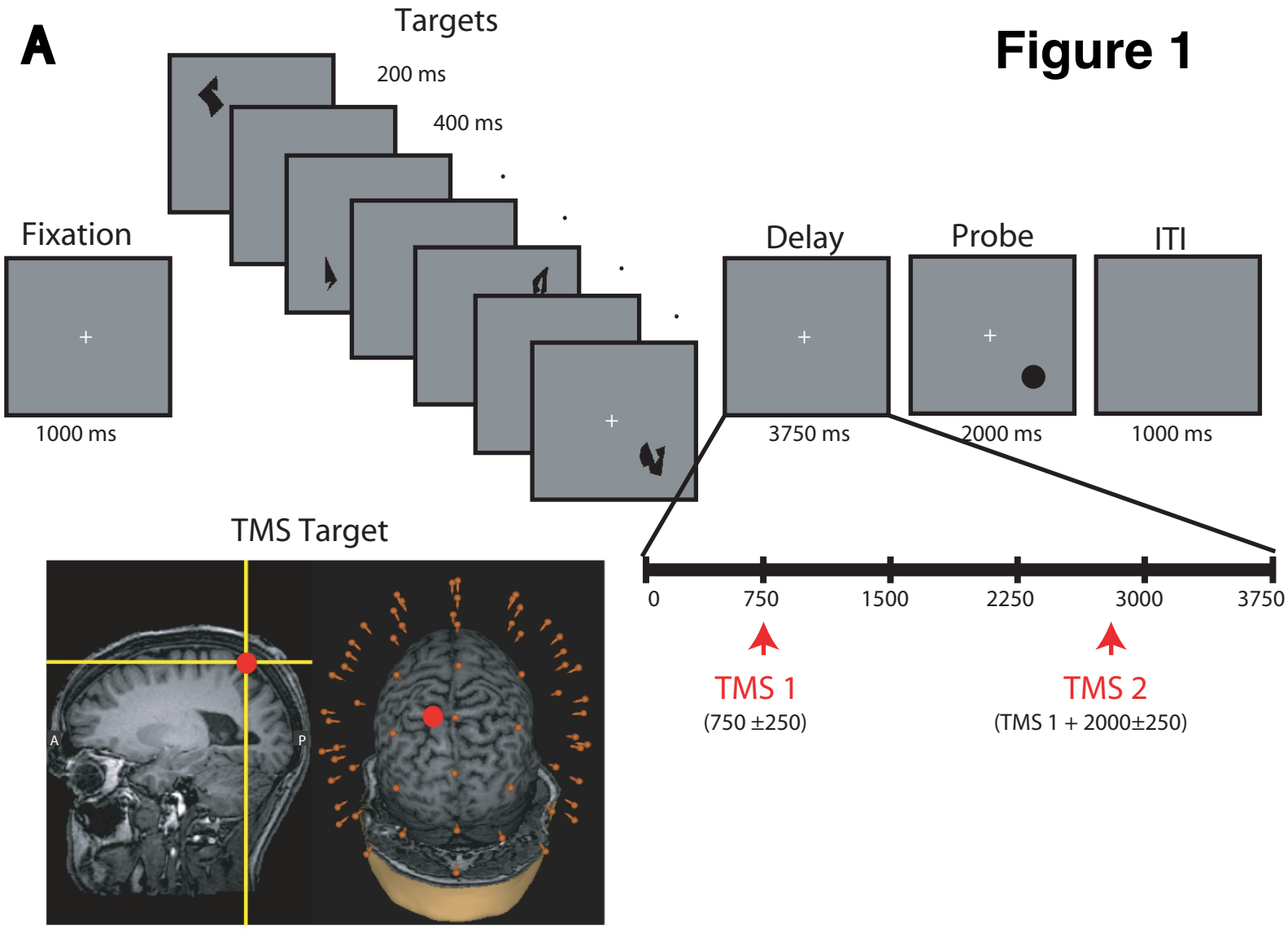
A
Targets
200 ms
400 ms
Fixation
1000 ms
Delay
3750 ms
Probe
2000 ms
ITI
1000 ms
TMS Target
A
P
0
750
1500
2250
3000
3750
TMS 1
(750 ±250)
TMS 2
(TMS 1 + 2000±250)

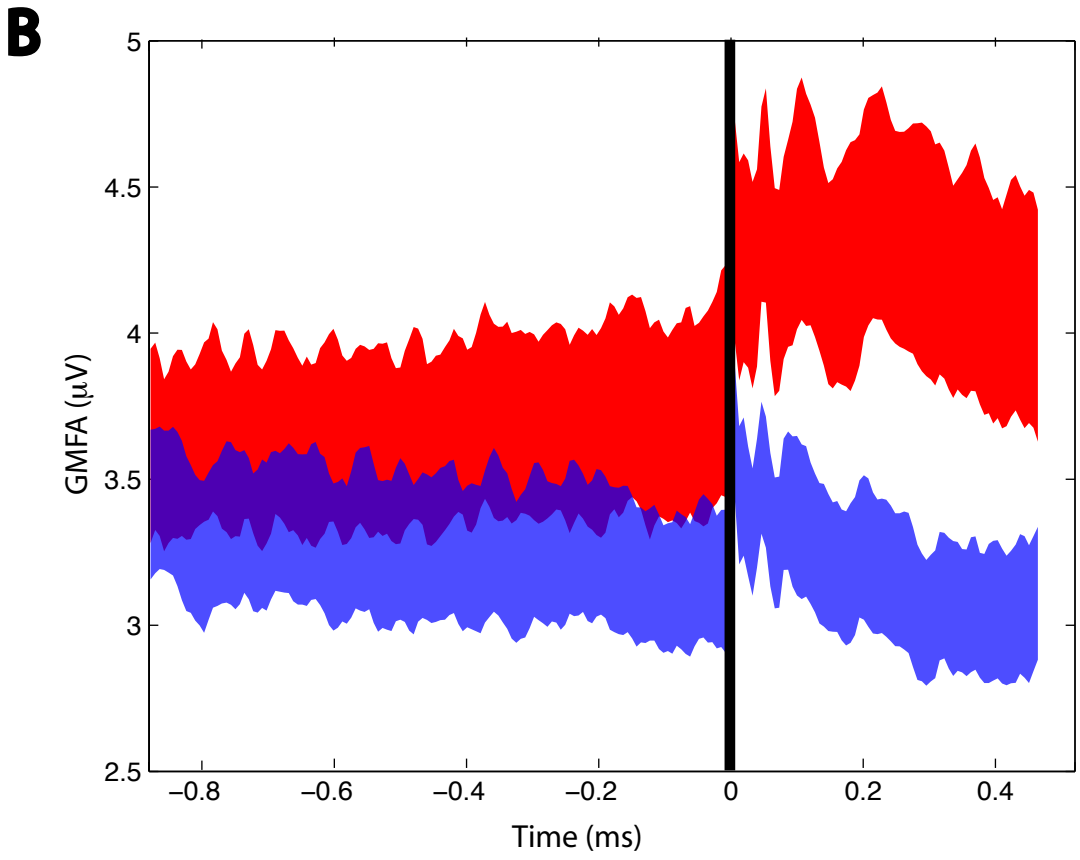
B
5
4.5
4
3.5
3
2.5
GMFA (μV)
−0.8
−0.6
−0.4
−0.2
0
0.2
0.4
Time (ms)

# Figure 2

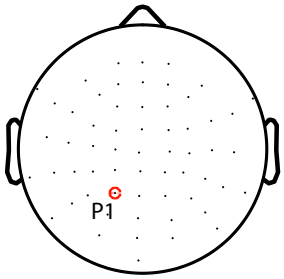
P1

**A**

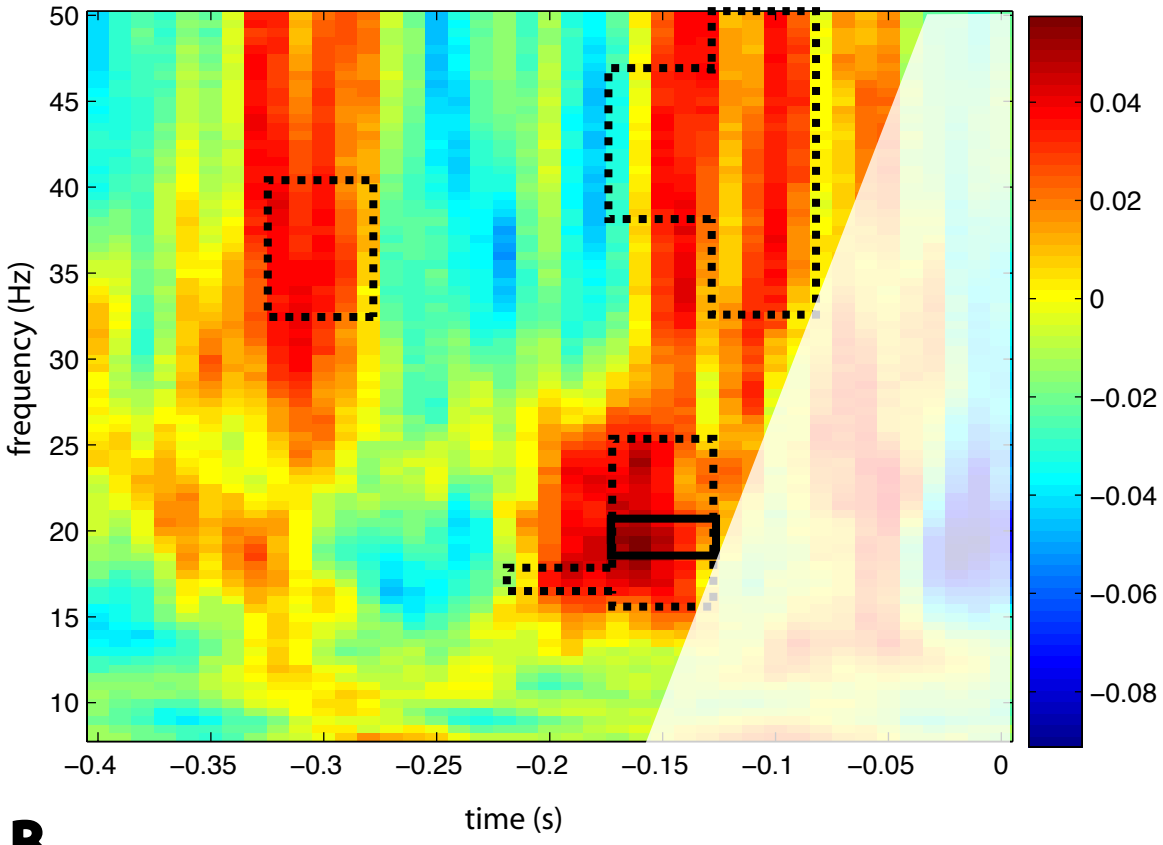
frequency (Hz)
time (s)
50
45
40
35
30
25
20
15
10
−0.4
−0.35
−0.3
−0.25
−0.2
−0.15
−0.1
−0.05
0
0.04
0.02
0
−0.02
−0.04
−0.06
−0.08

**B**

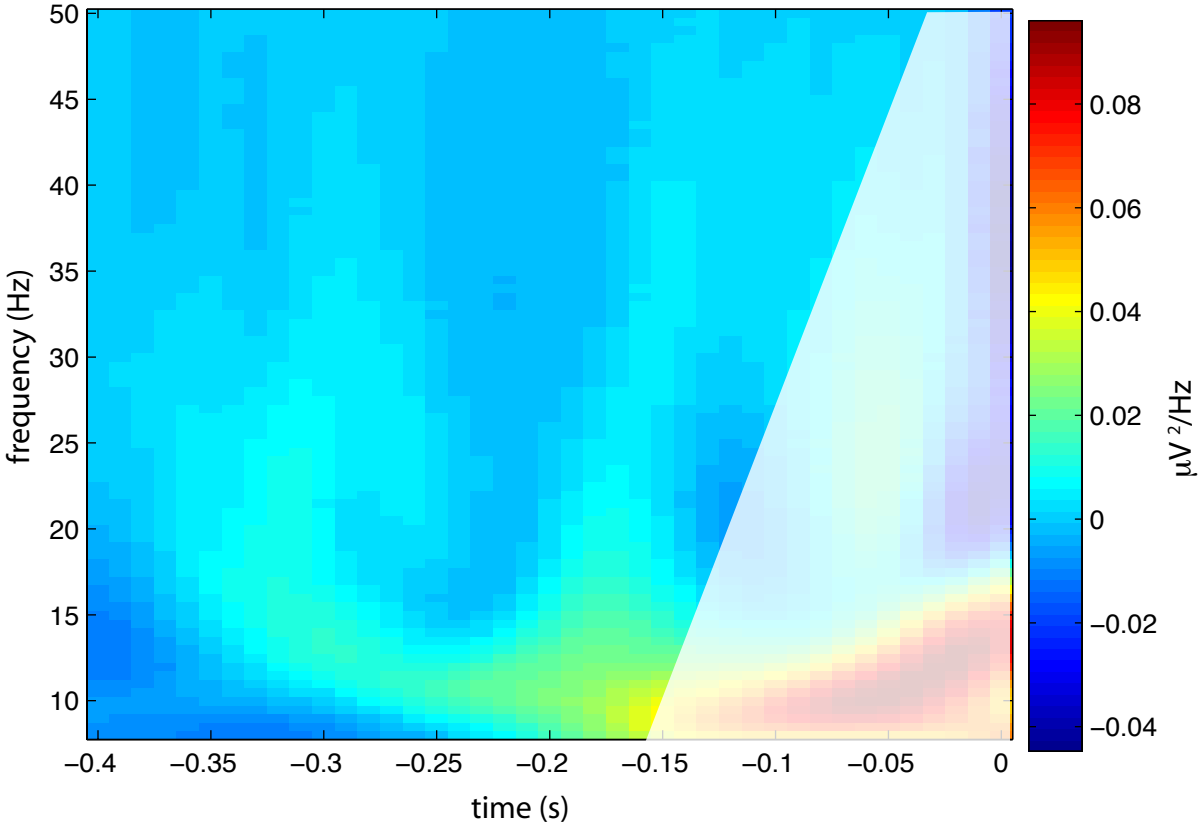
frequency (Hz)
time (s)
50
45
40
35
30
25
20
15
10
−0.4
−0.35
−0.3
−0.25
−0.2
−0.15
−0.1
−0.05
0
0.08
0.06
0.04
0.02
0
−0.02
−0.04
μV²/Hz

# Figure 3

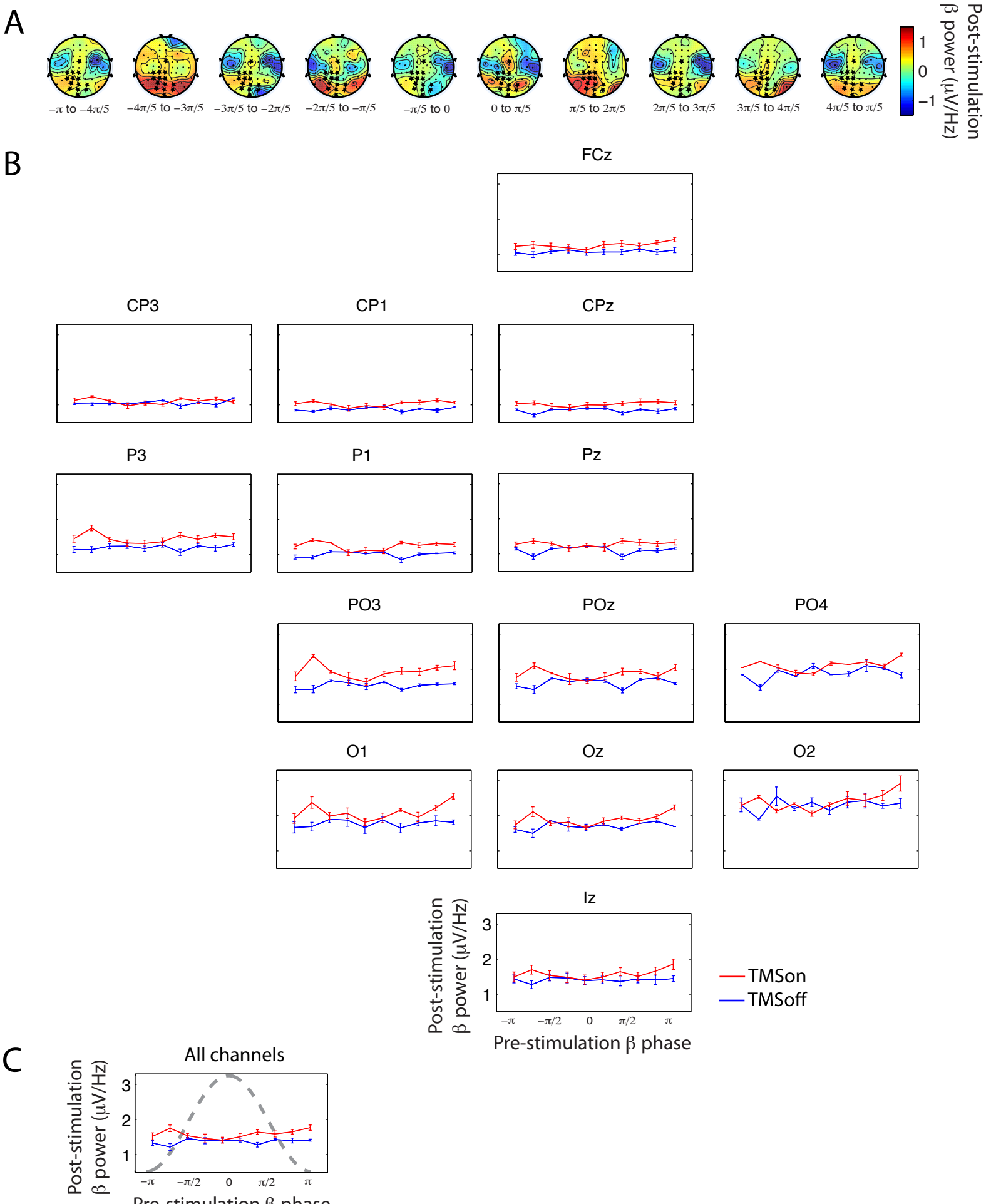
A
−π to −4π/5
−4π/5 to −3π/5
−3π/5 to −2π/5
−2π/5 to −π/5
−π/5 to 0
0 to π/5
π/5 to 2π/5
2π/5 to 3π/5
3π/5 to 4π/5
4π/5 to π/5
1
0
−1
Post-stimulation β power (μV/Hz)
B
FCz
CP3
CP1
CPz
P3
P1
Pz
PO3
POz
PO4
O1
Oz
O2
Iz
3
2
1
Post-stimulation β power (μV/Hz)
−π
−π/2
0
π/2
π
Pre-stimulation β phase
TMSon
TMSoff
C
All channels
3
2
1
Post-stimulation β power (μV/Hz)
−π
−π/2
0
π/2
π
Pre-stimulation β phase